

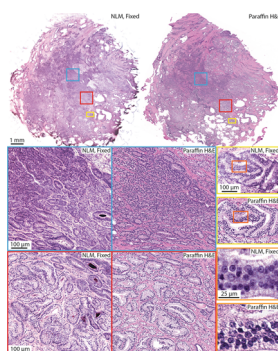
# INSIDE THE USCAP JOURNALS

<https://doi.org/10.1038/s41374-019-0291-0>

## MODERN PATHOLOGY

### NLM for real-time intraoperative imaging of prostate tissue

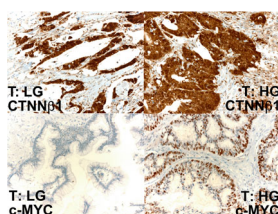
<https://doi.org/10.1038/s41379-019-0250-8>



Assessing intraoperative margins during surgical resection using H&E requires time and labor. Cahill et al. compared results obtained using nonlinear microscopy (NLM) of whole-mount unstained specimens with those obtained using traditional H&E. NLM images of unsectioned tissues were generated by two-photon (nonlinear) excitation of fluorophores, in which fluorescence is emitted from tissue only at the microscope focus, which avoided the need to cut physical sections. The investigators projected the NLM images in a color scale similar to that of H&E before performing corresponding H&E of fresh and fixed prostate specimens. Genitourinary pathologists assessed the pairs of images. Differences between the two types of images were noted, but interpretation of the NLM images did not require extensive training. NLM enabled visualization of key features of prostate tissue—normal architecture, benign conditions, and carcinoma—as well as Gleason patterns. The most significant advantage of NLM over H&E is the elimination of the embedding and cryotomomy/microtomy steps, allowing rapid assessment in an intraoperative environment.

### Genetic phenotypes of appendiceal mucinous neoplasms

<https://doi.org/10.1038/s41379-019-0256-2>

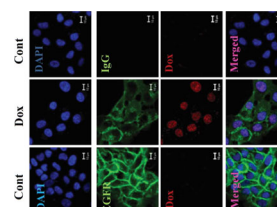


LaFramboise et al. used microdissection to obtain DNA samples from primary tumor cells, paired metastases, and peripheral blood mononuclear cells from patients with appendiceal mucinous neoplasms. Specimens of different grades were compared using an amplicon sequencing panel of 409 cancer-related genes. In the cohort of patients with high-grade tumors, there were significantly more DNA-damaging variants, although both cohorts contained damaging heterozygous germline variants (*catenin β1* and *notch receptor 1* and 4). High-grade tumors expressed higher levels of proto-oncogenes such as *MYC* and *death domain associated protein (DAXX)*, with damaging somatic variants in *TP53*. Ultimately, the investigators were able to profile the elements likely to be responsible for the aggressive phenotype of a high-grade tumor with activity driving cells toward dedifferentiation, proliferation, and migration. Larger patient cohorts could increase the statistical significance of this data to the point where they could be used in prognostic classification of appendiceal mucinous neoplasms.

## LABORATORY INVESTIGATION

### Cholesterol can regulate efficacy of doxorubicin

<https://doi.org/10.1038/s41374-019-0193-1>

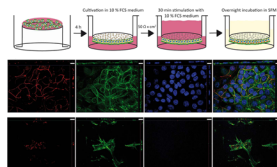


The interactions between patients' anti-cancer regimens and their other medications are still being evaluated. Yun et al. sought to evaluate the ways in which cholesterol-lowering statin drugs affected the efficacy of doxorubicin. Cholesterol has known roles in cell growth and cell signaling. In this study, downregulating 3-hydroxy-3-methylglutaryl coenzyme A reductase (HMG-CR) protein levels through inactivation of the EGFR/Src pathway not only reduced cholesterol levels as expected but also increased doxorubicin-induced cell death. A high-cholesterol diet attenuated the anti-cancer effects of doxorubicin in a tumor xenograft mouse model. More

data are to be collected to assess the relationship between serum cholesterol levels and HMG-CR expression in cancer tissue. The authors propose a new pathway—EGFR/Src/HMG-CR—that mediates doxorubicin-induced cell death. Thus, regulating cholesterol levels in patients undergoing doxorubicin treatment could enhance efficacy by decreasing the required dose while reducing side effects.

## The blood–brain barrier

<https://doi.org/10.1038/s41374-019-0250-9>



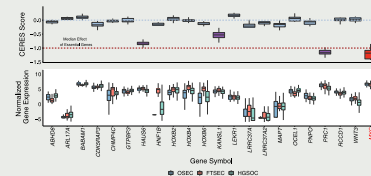
Lauer et al. generated a model of the blood–cerebrospinal fluid barrier using porcine choroid plexus (CP) epithelial cells to study granulocyte transmigration, levels of which are a hallmark of inflammatory events in the central nervous system. The group cultivated the CP cells on cell culture filter inserts containing a membrane with a pore size of 0.4  $\mu\text{m}$ . In previous attempts to represent the blood side of the barrier, the cells were grown on the lower face of a filter with a supporting membrane pore size of at least 3.0  $\mu\text{m}$ . With larger pores, the cells grow through the pores and cultivate a second layer on the upper face of the membrane. In this new model, the cells form continuous tight junctions and a strong barrier function, allowing improved assessment of porcine granulocyte transmigration across the barrier. Comparisons between this model and human-derived models are needed.

## nature.com/pathology

### New susceptibility genes for ovarian cancer

Gusev et al. performed both a transcriptome-wide association study of gene expression and splice junction usage and a genome-wide association study (GWAS) to identify susceptibility genes for high-grade serous ovarian cancer (HGSOC). In vitro assays for *CHMP4C*, one of 25 candidates identified in the transcriptome study, showed that the associated variant induces allele-specific exon inclusion. There was crossover between this study and target genes identified in 6 of 13 distinct GWAS regions, and the group identified 23 new candidate genes for susceptibility to HGSOC. Three of these genes—*KANSL1*, *HAUS6*, and *PRC1*—showed levels of essentiality, with *PRC1* showing levels similar to those of *MYC*, a known oncogenic marker for ovarian cancer. These new targets have implications in the clinic for heritability and diagnostics.

*Nature Genetics* 2019;51:815–823; <https://doi.org/10.1038/s41588-019-0395-x>

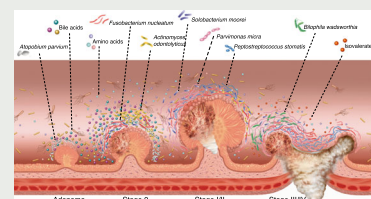


### Gut microbiome and metabolome for diagnosis of colorectal cancer

Fecal samples from 616 participants were assessed for taxonomic and functional characteristics of gut microbiota and metabolites. Yachida et al. made correlations between shifts in the microbiome/metabolome and cases of multiple adenomas and intramucosal carcinomas or more advanced lesions. Relative abundance of *Fusobacterium nucleatum* spp. was significantly elevated across stages of intramucosal carcinoma to more advanced stages.

*Atopobium parvulum* and *Actinomyces odontolyticus* were significantly increased in multiple adenomas and/or intramucosal carcinomas. Branched-chain amino acids, phenylalanine, and bile acids were also significantly elevated. The group concluded that they had sufficient data to discriminate cases of intramucosal carcinoma from the healthy controls, and that the telling shifts in microbiome and metabolome occur early enough to be potentially useful in diagnostic screening for colorectal cancer.

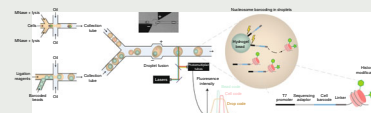
*Nature Medicine* 2019;25:968–976; <https://doi.org/10.1038/s41591-019-0458-7>



### Chromatin state heterogeneity in breast cancer

Grosselin et al. sought to assess the contribution of chromatin remodeling features to breast cancer heterogeneity and evolution using a high-throughput droplet microfluidics platform to profile chromatin landscapes of thousands of cells, at single-cell resolution. Chromatin-state signatures from patient-derived xenograft models of acquired resistance to systemic therapies in breast cancer (tamoxifen and capecitabine) were used to isolate a subset of cells within untreated drug-sensitive tumors that had lost the H3K27me3 chromatin signature, a known marker of stable transcriptional repression in genes known to promote resistance. The subset of cells affected seems small enough to have been obscured in bulk sequencing and analysis approaches. Therefore, the authors propose a new line of inquiry to assess single-cell immunoprecipitation followed by sequencing as a mechanism to assess chromatin heterogeneity, not only in cancer but also in other disease and healthy systems in which cell differentiation and development play a role in disease phenotype and cellular differentiation.

*Nature Genetics* 2019;51:1060–1066; <https://doi.org/10.1038/s41588-019-0424-9>



Emma Judson PhD contributed to these reviews.